North African mineral dust across the tropical Atlantic Ocean: Insights from dust particle size, radiogenic Sr-Nd-Hf isotopes and rare earth elements (REE)

Michèlle van der Does[a,*], Ali Pourmand[b], Arash Sharifi[b], Jan-Berend W. Stuut[a]

[a] NIOZ – Royal Netherlands Institute for Sea Research, Department of Ocean Systems, and Utrecht University, Texel, The Netherlands
[b] Neptune Isotope Laboratory, Department of Marine Geosciences, Rosenstiel School of Marine and Atmospheric Science, University of Miami, Miami, FL, USA

ABSTRACT

Large amounts of mineral dust are exported from North Africa across the Atlantic Ocean, impacting the atmosphere and ocean during transport and after deposition through biogeochemical processes. In order to characterize the isotopic signature of dust from different seasons and years, in relation to their bulk particle size, and to obtain a general idea of its provenance, Saharan dust was collected using subsurface sediment traps moored in the tropical North Atlantic Ocean in 2012–2013, and by shipboard aerosol collection during three trans-Atlantic research cruises in 2005, 2012 and 2015. The samples were analysed for radiogenic Strontium (Sr), Neodymium (Nd), and Hafnium (Hf) isotopes, rare earth element (REE; La-Lu) abundances and particle size. In addition, soil sediments from Mauritania, a potential source area, were analysed and compared to the Atlantic dust samples. The results indicate no relation between Sr and Nd isotopic compositions and dust particle size. In contrast, Hf isotopic compositions show a strong relation with particle size, associated to the so-called zircon effect. We explored alternative sources of lithogenic particles to the sediment traps such as Amazon River sediments. Our results reveal that the sediment-trap samples bear distinctly different geochemical signatures from sediments from the Amazon Basin and Amazon River tributaries, and confirm that the primary source of lithogenic particles is northern Africa. The collected dust samples show close relations to African dust aerosols collected at Barbados and samples from the Bodélé Depression, although differences between seasons are observed, which we relate to differences in source areas.

1. Introduction

The Sahara Desert in northern Africa is the world's largest dust source (Muhs, 2013), contributing up to 70% of all global annual dust emissions (Maher et al., 2010; Huneeus et al., 2011). In particular, the Bodélé Depression, located in the region of the Lake Chad Basin, is currently the largest single dust source, with the biggest dust export in the world (Koren et al., 2006; Washington et al., 2006), and appears to have been active for at least several hundred to thousands of years (Prospero et al., 2002; Armitage et al., 2015). Nevertheless, the contribution from the Bodélé Depression aerosols transported over the Atlantic basin arriving at Barbados in the Caribbean appears to be small (Pourmand et al., 2014; Bozlaker et al., 2018; Kumar et al., 2018). Most dust emitted from North African sources is transported westward across the Atlantic Ocean, with an estimated amount of 182 Tg between 30 °N and 10 °S every year (Yu et al., 2015). The emitted dust impacts both the atmosphere and the ocean, from affecting the atmospheric radiation

budget (Ryder et al., 2013) and acting as cloud condensation nuclei and ice nuclei (Wilcox et al., 2010; Atkinson et al., 2013), to the enhancement of the ocean's carbon cycle by delivering nutrients stimulating phytoplankton growth (Martin and Fitzwater, 1988), and by mineral ballasting of organic particles in the ocean (Armstrong et al., 2002; Bressac et al., 2014; Van der Jagt et al., 2018). Saharan dust can also transport viable spores, pathogens and microbes over great distances (Griffin, 2007), which can impact marine and terrestrial ecosystems (De Deckker et al., 2008), and be harmful to human health and increase mortality rates (Morman and Plumlee, 2014; Schweitzer et al., 2018).

Dust particle size and composition vary seasonally, and with the distance over which the dust is transported. Particle sizes decrease downwind as a result of more rapid gravitational settling of coarse-grained particles (Bagnold, 1941; Van der Does et al., 2016), while the mineralogical and isotopic composition of the deposited dust changes downwind by the preferential settling of heavier quartz and zircon particles closer to Africa (Pourmand et al., 2014; Korte et al., 2017). At
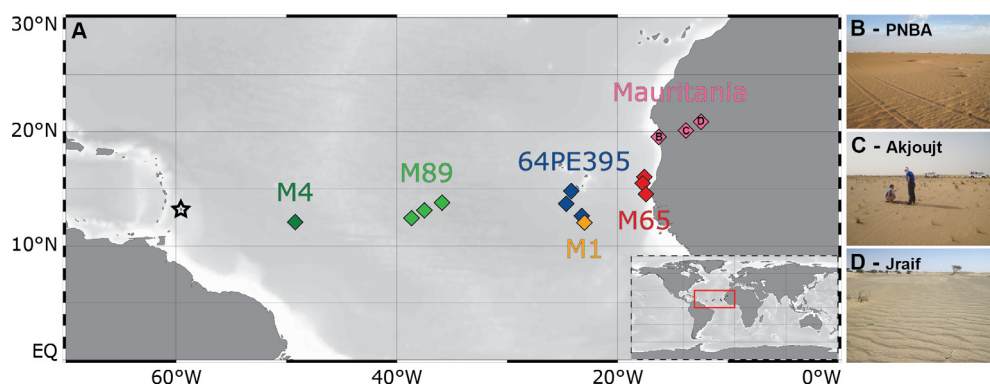
Fig. 1. A: Location of the samples used in this study in the North Atlantic Ocean: Sediment-traps M1 (12 °N, 23 °W) and M4 (12 °N, 49 °W); Soil samples from Mauritania; and average locations of aerosol samples collected during three research cruises: M65, M89 and 64PE395. The Caribbean island Barbados is indicated with a star. Photos of sample locations PNBA (B), Akjoujt (C) and Jraif (D) in Mauritania.

Barbados in the Caribbean, daily dust samples have been collected for over 50 years (Prospero et al., 1970; Prospero and Nees, 1977; Prospero and Lamb, 2003), making it one of the longest present-day dust records. Dust concentrations at this island peak during the summer months, related to the latitudinal movement of the Intertropical Convergence Zone (ITCZ). This leads to a northern displacement of the dust cloud over the Atlantic Ocean in summer, followed by a southward migration in winter (Nicholson, 2000). In addition, mineral dust is typically transported at low altitudes (< 3000 m) by the trade winds during the winter season, whereas the Saharan Air Layer (SAL) carries the dust at higher altitudes (> 5000 m) across the Atlantic during the summer (Stuut et al., 2005; Friese et al., 2016; Van der Does et al., 2016). The latitudinal and altitudinal seasonal shift of the dust-carrying atmospheric systems, in turn, results in a change of dust transport from different source areas and thus a seasonal change of dust composition (Pourmand et al., 2014; Friese et al., 2017).

Compositional characterization of trace elements and different isotope systems of mineral dust particles can yield information about the source area of the dust (Scheuvens et al., 2013), and selective processes during transport and deposition such as the sorting based on particle size and shape. Dust provenance identification can be aided by determining the mineralogical composition (Caquineau et al., 1998; Kandler et al., 2009, 2011; Friese et al., 2017), geochemical composition (Moreno et al., 2006; Muhs et al., 2007; Castillo et al., 2008; Bozlaker et al., 2018), identification of biomarkers (Schreuder et al., 2018), and radiogenic isotopes (Grousset and Biscaye, 2005; Meyer et al., 2011; Abouchami et al., 2013; Pourmand et al., 2014). The radiogenic Sr, Nd, Hf isotopes and the REE composition of aerosols at emission and deposition sites are shown to be particularly useful proxies for understanding changes in dust provenances and weathering regimes (Scheuvens et al., 2013; Pourmand et al., 2014). Most rare earth elements (REEs) show comparable values relative to the average composition of the upper crust, however the depletion or enrichment of several elements as a result of natural (e.g., chemical and physical weathering processes that lead to enrichment or depletion of heavy minerals such as zircon) or anthropogenic processes can be used as a tracer for source regions (Meyer et al., 2011, 2013; Scheuvens et al., 2013).

Previously, Pourmand et al. (2014) analysed Sr-Nd-Hf isotopes and REEs of Saharan dust collected in the Caribbean at Barbados between 2003 and 2011, and demonstrated seasonal shifts of dust sources and transport from the Sahara, as well as a systematic shift in nearly all geochemical proxies as a function of temporally variable dust plumes. Zhao et al. (2018) compared these distal dust samples to surface sediments from the Sahara and Sahel, and also demonstrated the seasonal variation of dust provenance. Here, we present the radiogenic Sr-Nd-Hf isotope and REE composition of Saharan dust collected during three trans-Atlantic research cruises and from submarine sediment traps moored in the tropical North Atlantic Ocean. Their geochemical characteristics will provide a better understanding of dust transported and

deposited over the open Atlantic Ocean. Alternative sources of lithogenic particles to the sediment traps from Amazon River sediments are investigated. By analysing the geochemical composition and combining them with particle-size data, we aim to shed light on the provenance of the lithogenic fraction in the sediment-trap samples of anomalously high depositional events. The data are compared to soil samples collected from Mauritania and to data from literature, to gain insights into the general provenance of the dust, whether that is North African or South American. Moreover, this dataset also allows for comparing the composition of dust particles collected from the atmosphere with those collected after sinking through the water column.

2. Material and methods

2.1. Sample collection

Saharan dust was collected at five mooring stations along a transatlantic transect, as described by Van der Does et al. (2016) and Korte et al. (2017). The transect consisted of four stations along 12 °N, and a fifth station at 13 °N, with two sediment traps moored at each station at 1200 m and 3500 m below sea level (BSL). The sediment traps consisted of 24 sampling bottles which were pre-programmed to sample at synchronous intervals of 16 days, from 19 October 2012 to 7 November 2013 (Stuut et al., 2012, 2013). For this study, five samples from three different time intervals were analysed from two sediment traps, moored at 1200 m below sea level at stations M1 (23 °W) and M4 (49 °W) (Fig. 1, Table 1). These are synchronous sample intervals #12 (13-04-2013–29-04-2013) and #24 (22-10-2013–07-11-2013) from both stations, which showed anomalously high deposition fluxes at M4 (Van der Does et al., 2016), and #9 (24-02-2013–12-03-2013) from M1, which is the sample with the largest dust flux from that station.

Aerosol samples were collected during three different research cruises in the tropical North Atlantic Ocean: FS Meteor Expedition M65 in June 2005 (Mulitza, 2005), FS Meteor Expedition M89 in October 2012 (Stuut et al., 2012), and RV Pelagia Expedition 64PE395 in January 2015 (Stuut et al., 2015) (Fig. 1, Table 1). Samples from these three cruises were picked to represent three different seasons (summer, autumn and winter) of three different years, to shed light on possible differences in provenance of the dust in various years, and to be compared to the dust found in the sediment traps. During all cruises, aerosol sampling was performed with an Anderson high-volume dust collector, mounted on the deck above the bridge of the ship. Dust was collected on letter-sized Whatman Type 41 filters under a protective cover. The samplers were equipped with a wind vane which switched off the sampler during winds blowing at an angle > 90° from the ship's heading. This was done to prevent contamination from the ship's exhaust behind the sampler (see e.g. Stuut et al., 2012).

Soil samples were collected at various sites in Mauritania, one potential source and transit area of mineral dust, during a field campaign in 2009. These are named PNBA, Akjoujt and Jraif (Fig. 1), representing

Table 1
Sample intervals, positions of sampling, and modal particle size of sediment-trap samples, shipboard-collected aerosol samples and Mauritanian soil sediments.

Sample ID	Sample type	sampling interval				location		modal grain size (µm)
		from		to		lat (°N)	long (°W)	
		date	time (UTC)	date	time (UTC)			
M1-U9	**Sediment trap**	2/24/2013		3/12/2013		12.00	23.00	12.40
M1-U12		4/13/2013		4/29/2013				13.61
M1-U24		10/22/2013		11/7/2013				18.00
M4-U12	**Sediment trap**	4/13/2013		4/29/2013		12.06	49.19	7.08
M4-U24		10/22/2013		11/7/2013				10.29
M65-D3	**Aerosol**	6/13/2005	7:30	6/14/2005	13:30	15.95	17.54 [*]	26.14
M65-D4		6/14/2005	15:30	6/16/2005	21:45	15.44	17.71 [*]	28.70
M65-D5		6/16/2005	22:00	6/18/2005	13:00	14.52	17.45 [*]	28.70
M89-F09	**Aerosol**	10/10/2012	9:09	10/11/2012	14:53	13.71	35.82 [*]	37.97
M89-F10		10/11/2012	14:53	10/12/2012	10:00	13.09	37.45 [*]	37.97
M89-F11		10/12/2012	10:00	10/12/2012	20:30	12.41	38.63 [**]	41.68
64PE395-F04	**Aerosol**	1/11/2015	21:30	1/12/2015	9:00	14.79	24.17 [*]	4.05
64PE395-F06		1/12/2015	11:25	1/12/2015	17:20	13.68	23.67 [*]	4.05
64PE395-F08		1/12/2015	22:43	1/13/2015	9:46	12.57	23.23 [*]	4.05
PNBA	**Soil sediment**	11/18/2009				19.47	16.27	
Akjoujt		11/19/2009				20.07	13.79	
Jraif		11/20/2009				20.86	12.43	

* Average location of sampling at sea during transits.

** Sampled during stationary interval.

potential dust sources. The PNBA sample was taken from large (10–20 m) yellow dunes in Parc National de Banc D'Arguin (PNBA; Fig. 1B). The Akjoujt sample was taken from a relatively flat landscape with small (10–40 cm) vegetated dunes, about 70 km northeast of Akjoujt (Fig. 1C). The Jraif sample was taken from a dried-up lake bed in an area with mostly dunes close to Jraif (Fig. 1D). Exact sampling locations are given in Table 1.

2.2. Particle-size analysis

The results of dust particle-size analysis of the samples from the sediment traps were presented by Van der Does et al. (2016) and cited here for comparison. The dust was isolated from the filters of the shipboard-collected aerosol samples collected during cruises M65 and M89 by rinsing with Milli-Q water to remove the dust. The three filters collected during cruise 64PE395 were ashed in a low-temperature asher (~100 °C) to remove the dust from the filters. Immediately prior to grain-size analysis, a few drops of 0.1 M sodium pyrophosphate ($Na_4P_2O_7$ $10H_2O$) was added to the sample to ensure complete disaggregation of the particles. Particle-size distributions were obtained with a Coulter laser diffraction particle size analyser (LS13 320), equipped with a micro liquid module (MLM) as described by Van der Does et al. (2016). The samples were homogenized during analysis by a magnetic stirrer, and the influence of air bubbles was minimized using degassed water. This resulted in particle sizes ranging from 0.375 to 2000 µm, distributed over 92 size classes.

2.3. Radiogenic Sr-Nd-Hf systematics and REE composition

Prior to radiogenic analysis, the samples were ashed in a quartz crucible at 750 °C to remove all the organics, and were subsequently homogenized by grinding in an opal mortar and pestle. The two largest sediment-trap samples (M4-U12 and M4-U24) were split in two, of which one half the bulk sample and the other half the lithogenic fraction was analyzed. To isolate the lithogenic fraction (< 10% of bulk sample), the marine sediment-trap samples were treated to remove all biogenic constituents. This was performed by a sequential leaching procedure in several steps, based on the protocol described by Handley et al. (2013). First, the sample was rinsed with Milli-Q water and centrifuged. Next, 1 M sodium acetate (NaAc) in 25% acetic acid (HAc) were added to the sample to remove carbonates. Amorphous and

crystalline Fe- and Mn-oxides, which can adsorb dissolved REEs from the ocean (Tachikawa et al., 1997), were removed by adding 0.04 M hydrolaxamine hydrochloride ($NH_2OAH·HCl$) and nitric acid (HNO_3). Finally, biogenic silica was removed by adding 2 M sodium carbonate (Na_2CO_3), and samples were placed in an oven at 85 °C for 5 h. Every leaching step was followed by several rinsing and centrifuging steps. The samples were subsequently dried in an oven at 80 °C. No specific size fractions were isolated before geochemical analysis.

All samples were subsequently prepared following the method described in detail in Pourmand and Dauphas (2010), Pourmand et al. (2012, 2014). Briefly, the samples were fused with $LiBO_2$ alkali flux at 1070 °C and added to 6 M HNO_3 to ensure complete dissolution of refractory minerals. Radiogenic Sr, Nd, Hf isotopes and REEs were separated by a three-stage extraction chromatography scheme devised for high-precision isotope and elemental analysis on a Thermofisher Scientific Neptune Plus multi-collector inductively coupled plasma mass spectrometer (MC-ICPMS) at the Neptune Isotope Lab, University of Miami. To check for possible contamination, procedural blanks were processed and analyzed. Unless otherwise stated, the uncertainties on isotope ratios reported herein are at the 95% confidence interval. Variations in $^{143}Nd/^{144}Nd$ and $^{176}Hf/^{177}Hf$ are reported as εNd and εHf, expressed as deviations from the chondritic uniform reservoir (CHUR) values of 0.512630 ± 0.000011 and 0.282785 ± 0.000011, respectively (Bouvier et al., 2008). The abundances of REEs were normalized to the mean of Post-Archean Australian Shale (PAAS), as described by Pourmand et al. (2012). The ratio of Lanthanum over Lutetium (La/Lu) is given, to represent the extent of light REE (LREE) over heavy REE (HREE) fractionation, which is related to the source rock composition as a function of its geochemical evolution through time. LREE are less compatible than HREE during partial melt, leaving the melt enriched in LREE and the residue in HREE, which can be used to discern source rocks of mantle and crustal origin. Sm-Nd model ages are also used for this purpose, and represent the crustal residence age of the source rocks. The rock ages are the result of the weakly radioactive ^{147}Sm, which decays into ^{143}Nd, and the crustal ratios of $^{143}Nd/^{144}Nd$ (Elderfield and Greaves, 1982; Elderfield, 1988). The $^{147}Sm/^{144}Nd$ ratio of continental crust is generally lower than oceanic crust (Elderfield, 1988), and the difference becomes larger for rocks with younger ages. The Sm-Nd model ages are based on nominal value of 0.51316 for $^{143}Nd/^{144}Nd$ of depleted mantle and modern $^{147}Sm/^{144}Nd$ of 0.2137 (Goldstein et al., 1984; Grousset et al., 1988). The anomalies for Cerium

and Europium are calculated according to the following relationships, normalized to the mean values of La-Lu for Post Archean Australian Shale (PAAS; Dauphas and Pourmand, 2015):

$$Ce/Ce^* = Ce_N/(La_N^{0.48} \times Pr_N^{0.52}) \tag{1}$$

$$Eu/Eu^* = Eu_N/(Sm_N^{0.45} \times Gd_N^{0.55}) \tag{2}$$

Positive anomalies (> 1) mean Cerium and Europium are enriched, while negative anomalies (0–1) indicate they are depleted relative to their trivalent REE neighbors. Ce and Eu anomalies of 1 means that all three REEs have a crust-like composition (Sholkovitz, 1993). As Ce and Eu can carry different charges than their normal trivalent charge (+4 and +2, respectively), this can lead to distribution anomalies relative to the trivalent REEs (Elderfield and Greaves, 1982; De Baar et al., 1985; Elderfield, 1988). Ce can be preferentially incorporated in zircon minerals (Thomas et al., 2003) and Eu in plagioclase minerals (Weill and Drake, 1973; Elderfield, 1988), leading to enrichments of these elements if these minerals are more abundant. Ce anomalies can also be affected by oceanic redox conditions, and Eu anomalies by hydrothermal input (Elderfield, 1988), in the case of the sediment-trap samples.

3. Results

3.1. Dust particle size

The sample information, sampling day and time as well as samples' modal grain size (μm) data are presented in Table 1. Particle-size distributions of the sediment-trap samples show that in general, particles deposited at M1 close to the east coast of North Africa are coarser-grained compared to samples from M4 at the more distal location (Fig. 2A; Table 1). This finding is intuitively logical as coarser-grained wind-blown particles are deposited closer to the source (Van der Does et al., 2016). In addition, Van der Does et al. (2016) showed that seasonal changes in dust export exert control over the particle-size distribution of the dust, with coarser-grained particles in summer compared to winter. The sediment-trap samples collected in autumn (sample interval #24) are coarser-grained than the samples collected in spring (#9 and #12). In contrast, however, the shipboard-collected aerosol samples do not show the typical downwind decrease in particle size as expected. Samples from M65 and M89 are similar in particle size, but very different in sampling location. The samples from M89 were not expected to be coarsest as they were collected farthest from their north-African source (Fig. 1). Samples collected during 64PE395 have the smallest dust particles, and show the highest symmetry. The relative enrichment of coarse particles to the distributions of M89 and M65 could be due to the strength of the winds and dust events. Indeed, these samples were collected during summer (M65) and autumn (M89), when wind strengths are higher, and the dust is transported at greater altitudes within the SAL (e.g. Chouza et al., 2016). For the samples

collected during 64PE395, the ratio Median/Modal grain size—reflecting the difference between the most occurring value (mode) and the middle value (median)—is highest (~0.90), and thus the most similar, followed by the samples collected during M89 (~0.85) and M65 (~0.69). Both the samples collected in spring (#12) by the sediment traps at M1 and M4 (solid lines) and the shipboard-collected aerosols from M89 show a "shoulder" on the coarse end of the grain-size distribution (Fig. 2). These coarse-grained particles may mostly include mica particles, which have a different aerodynamical behavior due to their platy shape than more spherical quartz particles of similar diameter (Stuut et al., 2005; Van der Does et al., 2016), although the latter are also clearly present in the samples (Van der Does et al., 2016).

3.2. Radiogenic isotopes

Isotopic values for radiogenic Strontium, Neodymium and Hafnium are reported in Supplementary Table 2. $^{87}Sr/^{86}Sr$ values for the sediment-trap samples range between 0.718942 ± 0.000011 (M4-24) and 0.723324 ± 0.000013 (M1-24) (Fig. 3A). The shipboard-collected aerosol samples have lower $^{87}Sr/^{86}Sr$ values, averaging 0.713449 ± 0.0032, with the samples from M65 being the least radiogenic, and collected closest to the source. The Mauritanian sediments have Sr isotopic values similar to the sediment-trap samples except for the sample collected near Akjoujt, which is considerably more radiogenic than any of the samples or the source regions (Fig. 3B; $^{87}Sr/^{86}Sr = 0.745105 \pm 0.000011$).

The εNd values of the sediment-trap samples and the shipboard-collected aerosol samples cluster between -11.2 ± 0.26 (64PE395-F04) and -14.0 ± 0.11 (M1-U24), with mostly overlapping uncertainties (Fig. 3A). The sediment-trap samples collected at M1 have slightly lower εNd values (average −13.7 ± 0.62) than samples collected at M4 (average −12.8 ± 0.13). The Mauritanian sample Akjoujt also has a considerably lower εNd value (−20.0 ± 0.17) and falls well outside any source-region ranges previously reported (Fig. 3B).

The Hf isotopic composition of the samples shows higher εHf values for finer-grained dust samples, and decreasing values for coarser-grained samples (Fig. 4A; Supplementary Table 2). Sediment-trap samples from the most proximal station M1 have less radiogenic εHf values ranging from −17.2 ± 0.41 (M1-U24) to −15.3 ± 0.3 (M1-U9), with the coarsest sample having the lowest εHf value (M1-24) and the finest sample the highest (M1-09). These samples plot along the igneous rock array (Fig. 4A). Samples collected at M4 have relatively more radiogenic εHf values, with the coarsest sample (M4-24) having the lowest εHf value (−12.8 ± 0.98) and the finest sample (M4-12) the highest (−9.3 ± 0.68). These data plot between the igneous rock array and the zircon-depleted sediment array (Fig. 4A). Shipboard-collected aerosols of M65 have the least radiogenic εHf values and plot closest to the zircon-bearing sediment array. These samples are among the coarsest aerosol samples and are collected closest to the source of all
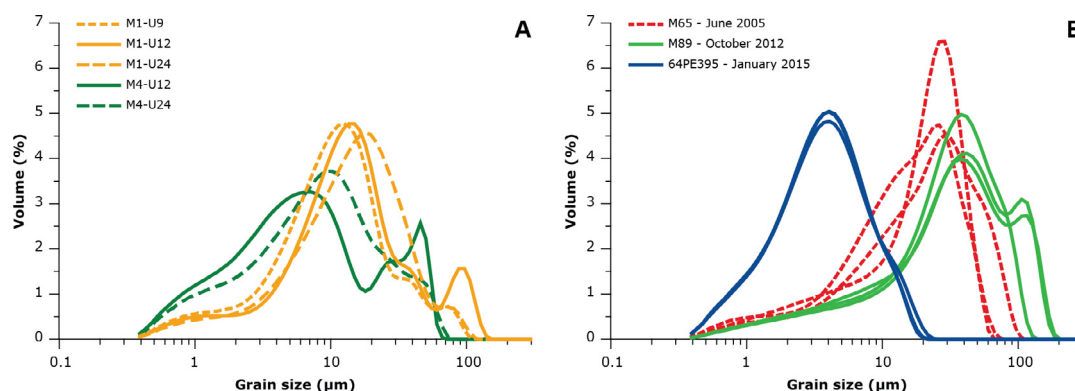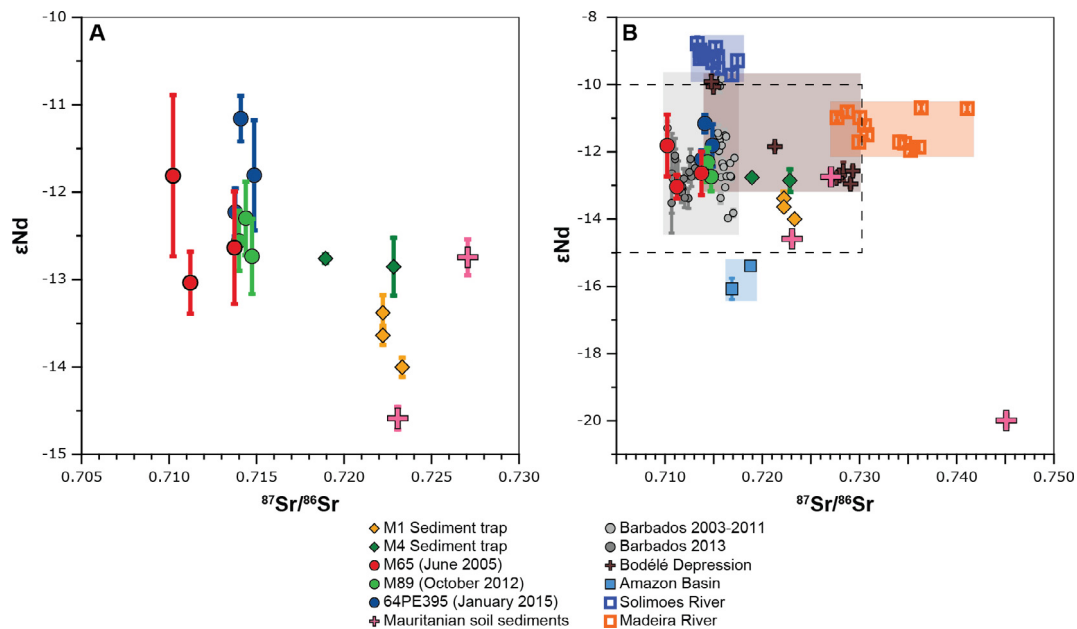

Fig. 2. Grain-size distributions of the A: Sediment-trap samples (Van der Does et al., 2016), and B: Shipboard-collected aerosol samples.
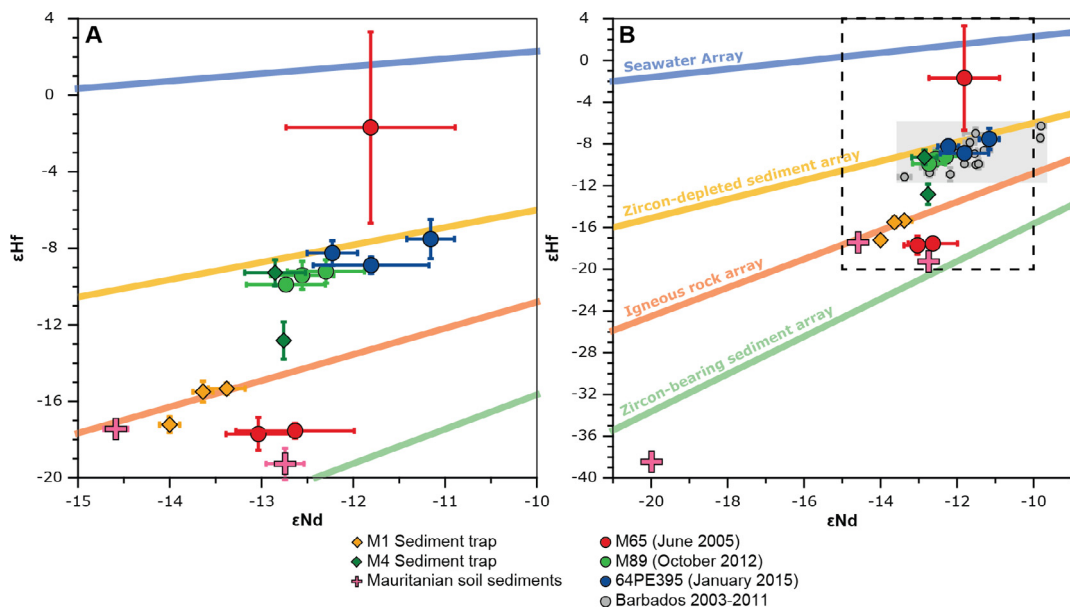
Fig. 3. Radiogenic Sr and Nd isotopes. A: Samples from sediment traps, shipboard-collected aerosols and Mauritanian sediments. B: The data are compared to published data: Aerosols collected on Barbados (Pourmand et al., 2014), sediments from the Amazon Basin, the Bodélé Depression in Chad (Abouchami et al., 2013), and suspended sediment load from the Solimoes and Madeira Rivers (Viers et al., 2008). Error bars define 95% confidence intervals, which for Sr is smaller than the size of the symbols.

the samples. Sample M65-D3 is an exception, with a highly radiogenic εHf value of −1.7 ± 5.00, albeit with a large uncertainty. Aerosol samples of M89 and 64PE395 plot close to the zircon-depleted sediment array, in the same range as the M4 sediment-trap samples. The Mauritanian sediments have values similar to the most proximal sediment-trap samples at M1, and the shipboard-collected aerosol samples of M65 (Fig. 4A).

3.3. Rare earth elements

The REE patterns for the sediment-trap samples show an enrichment for Eu (Fig. 5A), with Eu anomalies ranging between 1.12 and 1.16

(Fig. 6A; Supplementary Table 3). These samples are also slightly enriched in heavy REEs (HREE, Gd-Lu), with ΣHREE values ranging between 6.4 and 7.9. The shipboard-collected aerosol samples have similar REE patterns as the sediment-trap samples, but lack the HREE enrichment (Fig. 5B). These samples also show larger Ce anomalies, averaging 1.06, 1.04 and 1.10 for M65, M89 and 64PE395 samples, respectively (Fig. 6A). Eu-anomalies are very similar for both the sediment-trap samples (average 1.14) and the shipboard-collected aerosol samples (average 1.17), but Eu anomalies for two of the Mauritanian sediments are elevated; 1.18 and 1.56. Contrastingly, the REE patterns of the Mauritanian samples look very similar to the sediment-trap samples (Fig. 5A), with ΣHREE values ranging between 1.79 and 2.82,

Fig. 4. Radiogenic Hf and Nd isotopes. A: Samples from sediment traps, shipboard-collected aerosols and Mauritanian sediments. B: The data are compared to aerosols collected on Barbados (Pourmand et al., 2014). Seawater, sediment and rock arrays are defined by Bayon et al. (2009). Error bars define 95% confidence intervals.
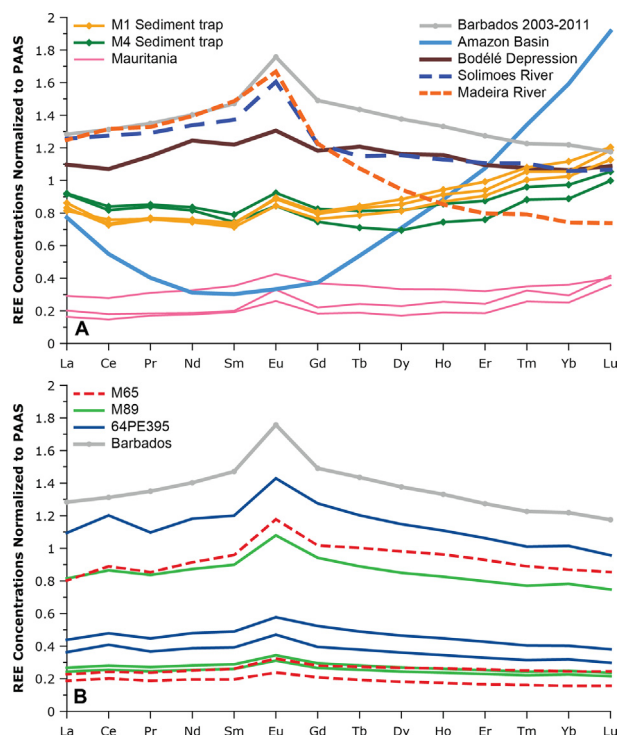
Fig. 5. PAAS-normalized REE concentrations of samples from sediment traps and Mauritanian sediments (A) and shipboard-collected aerosols (B). The data are compared to published data: Aerosols collected on Barbados (Pourmand et al., 2014), sediments from the Amazon Basin, the Bodélé Depression in Chad (Abouchami et al., 2013), and suspended sediment load from the Solimoes and Madeira Rivers (Viers et al., 2008), also normalized to PAAS.

and Eu anomalies ranging between 1.39 and 1.56. (Fig. 6B).

Sm-Nd model ages are highest for the Mauritanian sediments (1.9–2.5 Ga), and similar for the sediment-trap samples (1.6–1.8 Ga) and shipboard-collected aerosol samples (1.7–1.9 Ga) (Fig. 6D; Supplementary Table 3), indicating that the age of the source rock is the same for the latter two. However, these are model ages and their relative values are more meaningful than the absolute ages. Their distinction is clearer in combination with La_N/Lu_N values, which is higher for the shipboard-collected aerosol samples (up to 1.22) than for the sediment-trap samples (0.68–0.92) (Fig. 6C). The sediment-traps show similar values, close to the aerosol samples. The sediments collected at Jraif from Mauritania most closely resembles the dust samples.

4. Discussion

4.1. Relation between Strontium and particle size

Several studies have reported that Sr isotopes in particular maybe prone to grain-size dependence in their isotope composition (Dasch, 1969; Meyer et al., 2011). This is in turn related to the mineralogy, given that elemental Sr is preferentially enriched in minerals of low density and high buoyancy. Specifically, fine fractions are expected to have more radiogenic Sr isotopic values as these are usually composed of particles that are more prone to weathering such as clay minerals and micas (Feng et al., 2009), which have higher Rb/Sr ratios, resulting in more radiogenic $^{87}Sr/^{86}Sr$ compositions for fine-grained particles (Feng et al., 2009; Meyer et al., 2011; Aarons et al., 2013). Contrary to this general expectation, however, the dust samples that were measured in this study do not exhibit a notable grain-size dependence between samples with different modal particle sizes with respect to Sr isotopic values (Fig. 7A). If particle size was the only variable affecting the Sr isotopic composition of the samples, one would expect more radiogenic

values at M4 with finer-grained particles (7.1–10.3 μm). However this is not the case for the dust of different sizes at the different stations, nor between the individual samples at M1 (12.4–18.0 μm). Only at M4 does the finer-grained dust sample show more radiogenic Sr values than the coarser-grained sample. In the case of the samples studied here, the Sr isotopic values are therefore likely the result of a provenance signal that appears to dominate over the influence of the grain-size effect. As the Sr isotopic values of the sediment-trap samples are mostly > 0.720, a source in the west of northern Africa can be expected (Scheuvens et al., 2013).

For the shipboard-collected aerosols, the lack of relation between particle size and distance to the source may be related to the influence of seasonality, inter-annual variability and specific dust events, which can be related to differences in wind speed and changes in the provenance of the dust particles. Indeed, samples collected during 64PE395 have the smallest dust particles, related to finer-grained dust transport during winter, while coarser-grained dust is observed in summer and fall, in agreement with previous findings from sediment-trap samples along the sampled transect (Van der Does et al., 2016). The shipboard-collected aerosol samples do not show significant variation in Sr isotopic values, despite the particle size being very different (Fig. 7A), also among the individual samples of the different sampling campaigns. This is contrary to previous findings of a strong relation between particle size and Sr isotopic composition, although this was established for size-separated fractions of dust (Dasch, 1969; Meyer et al., 2011). Two of the shipboard-collected aerosol samples of M65, closest to the African coast, are exceptions and have the lowest Sr isotopic values (Fig. 3A). Although these samples are not the coarsest, they may have relatively more quartz particles than clay particles due to their proximal location to the source, influencing radiogenic Sr values. Alternatively, a relatively larger contribution of less radiogenic carbonates could have influenced the radiogenic Sr values, although we would expect the three samples of M65 to be similar in composition, as these were collected very close to each other, both geographically as well as temporally. The "shoulder" at the coarse end of the grain-size distributions, possibly related to a larger amount of platy mica particles, can also influence the isotopic signature, although this is not clear for the samples presented here. In addition, an aspect of the transport distance that may be overlooked is that the samples closer to the west-African coast are seemingly closer to their possible source areas, but the dust found in these samples could originate from sources much further inland.

4.2. Relation between Neodymium and particle size

In contrast to Sr isotopes, Nd isotopes are not expected relate to the dust's particle size (Feng et al., 2009; Meyer et al., 2011), related to the different geochemical behavior of elemental ^{87}Sr and its parent isotope ^{87}Rb, and a more similar behavior between ^{143}Nd and its parent isotope ^{147}Sm, respectively. Sr is more easily lost from minerals during weathering processes than Rb, and Sm and Nd show similar responses to weathering (Feng et al., 2009). Indeed, no relation between the Nd isotopic values and the dust's modal grain size is observed (Fig. 7B). The low Nd isotopic values of the shipboard-collected aerosols and sediment-trap samples also point to a source area of the dust in a more western region of northern Africa (Scheuvens et al., 2013). The Mauritanian sediments show similarities to the sediment-trap samples, except for the sample from Akjoujt, which is different in all isotope systems and which may therefore not be representative of the average composition of the source soil. Nevertheless, it must be noted that highly radiogenic Sr values in combination with less radiogenic Nd isotopic values have been reported for Mauritania (Scheuvens et al., 2013). However, the interpretation of these soil samples as long-range mineral dust should be done with caution, considering potential aerosol samples might be substantially different than the soil sediments (Pourmand et al., 2014). We also note that these particles can inherently have very different particle-size distributions, and mineral and
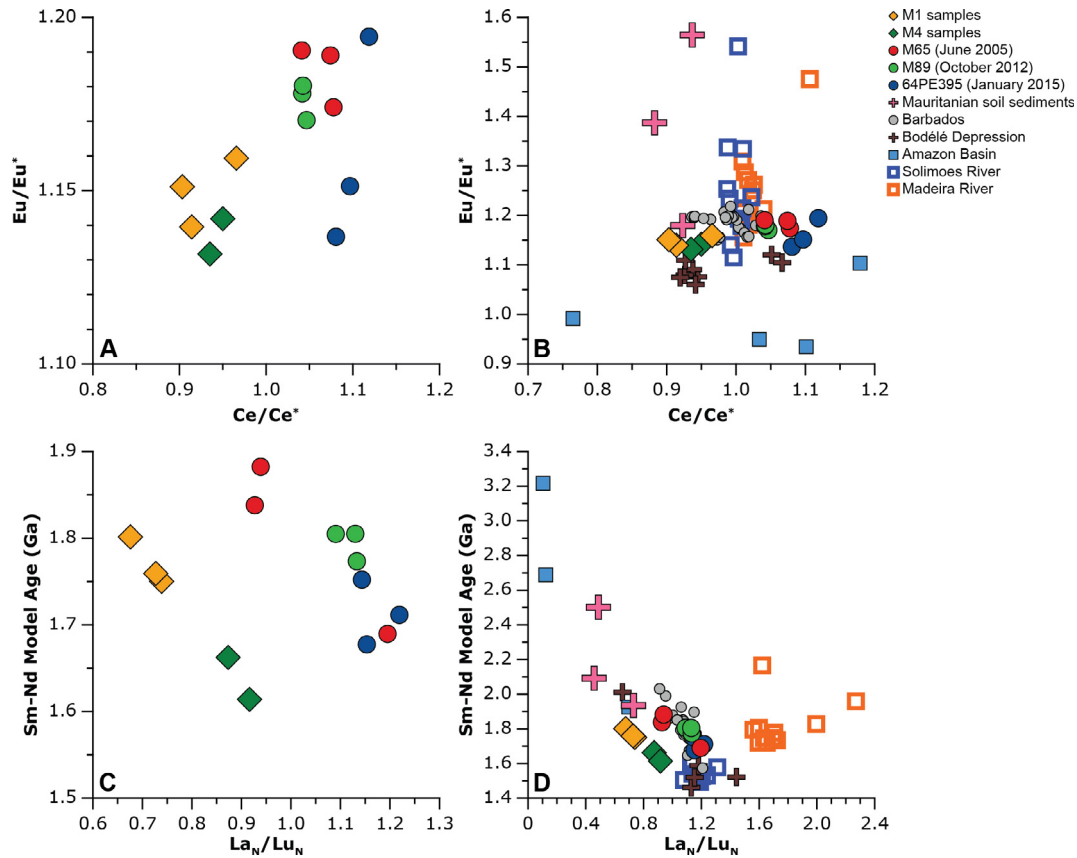
Fig. 6. A: Eu- and Ce-anomalies of samples from sediment traps and shipboard collected aerosols. B: The data including Mauritanian sediments, and compared to published data: Aerosols collected on Barbados (Pourmand et al., 2014), sediments from the Amazon Basin, the Bodélé Depression in Chad (Abouchami et al., 2013), and suspended sediment load from the Solimoes and Madeira Rivers (Viers et al., 2008). C and D: Sm-Nd model age and La_N/Lu_N of the same samples.

chemical composition as a result from sorting during dust generation, transport and deposition. This sorting occurs as the dust is transported in different ways during different seasons, at different altitudes, which results in the falling out of different minerals affecting the total composition of the deposited dust and the remaining airborne dust (Scheuvens et al., 2013). These findings place more emphasis on the need to characterize erodible soil with high potential for generating airborne particles in potential source regions to allow for a consistent comparison of dust particles between source and sink, based on their geochemistry, as Zhao et al. (2018) did for four potential source regions in northern Africa.

4.3. Relation between Hafnium and particle size

The grain-size dependence of Hf isotopes is the result of gravitational settling of zircons during transport, and is known as the "zircon effect" (Patchett et al., 1984; Aarons et al., 2013). Zircon minerals typically have low $^{176}Hf/^{177}Hf$ isotopic ratios due to their extremely low Lu/Hf ratios, which results from Lu exclusion and Hf incorporation in the crystal structure of zircons (Hoskin and Schaltegger, 2003). Heavier zircon particles are deposited close to the source during atmospheric transport, changing the Hf isotopic composition of dust aerosols with increasing transport distance towards more radiogenic Hf isotopic values (Patchett et al., 1984; Aarons et al., 2013). The more radiogenic Hf
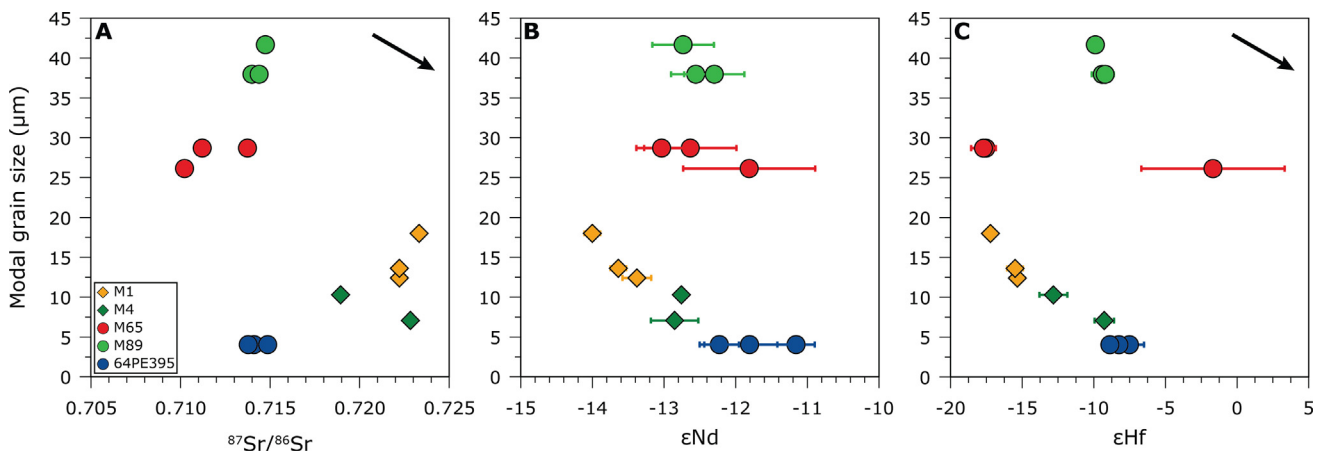

Fig. 7. Relation between Sr-Nd-Hf isotopes and dust modal grain size. Arrow indicates the expected relation between size and isotopic composition.

isotopic values for fine-grained dust samples and lower $^{176}Hf/^{177}Hf$ for coarser-grained samples is observed for all the sediment-trap samples (Fig. 7C), in combination with the fine-grained Barbados samples that have high εHf values. These samples all plot close to the zircon-depleted sediment array (Fig. 4B). Here it seems that the zircon effect for these samples is superimposed on the isotopic signature resulting from different dust provenances. The low εHf values for the samples collected during M65 can be similarly explained as a relative enrichment of zircons, as these are generally deposited and collected close to the source. The more distal samples collected during the M89 and 64PE395 sampling campaigns have more radiogenic Hf isotopic values close to the zircon-free sediment array, similar to the Barbados and M4 samples.

4.4. Comparison to dust collected at Barbados

To examine the influence of long-range transport, the presented data are compared to atmospheric dust collected at Barbados between 2003 and 2011, in 2007 and in 2013, with Sr isotopic values averaging 0.715804 ± 0.0026 (Pourmand et al., 2014), 0.720120 ± 0.0034 (Kumar et al., 2018) and 0.711754 ± 0.0015 (Bozlaker et al., 2018), respectively. These are similar to the shipboard-collected aerosols, but less radiogenic than the deposited dust as found in the sediment-trap samples (Fig. 3B). The dust mean particle size for mineral dust collected at Barbados is much finer-grained (smaller than 5 µm; Li-Jones and Prospero, 1998) than the samples analyzed for this study. As a result, one would expect the highest $^{87}Sr/^{86}Sr$ values, in line with the expected relation between particle size and Sr isotopic composition. Nevertheless, these values appear to be among the least radiogenic, and the Sr isotopic composition are more likely the result of differences in dust provenance (that is related to the age of the source rocks and the mineralogical composition). Dust collected at Barbados in 2013 by Bozlaker et al. (2018) is expected to be similar to the dust collected in the same period by the sediment traps. However, these dust samples collected at Barbados have systematically lower Sr isotopic values, and therefore are not necessarily related to dust provenance only, and thus possibly related to transport distance, which affects dust particle size and mineralogy. The reason why this is not clearly present for the shipboard-collected aerosol samples is due to the different years and season of dust collection, and therefore overprinted by the differences in dust provenance. The lack of a clear relationship between Sr isotopic composition and particle size of the shipboard-collected aerosol samples could also result from a strong Sr signal from one particular size class within the sample, thereby dominating the Sr signal from over the other size classes. This also illustrates the significance of source-related signals in contrast to size-controlled signatures of dust particles. Seasonal changes in isotopic signature related to differences in provenance were also found by Zhao et al. (2018), who compared the isotopic signature of clay-sized sediments from source areas to long-range transported dust to Barbados during 2013 and 2014 dust seasons, and by Kumar et al. (2018), who compared dust collected at the proximal Cape Verde Islands to dust collected at Barbados. The latter group found more variable Sr and Nd isotopic compositions during winter at the proximal Cape Verde Islands, reflecting changing dust provenance (Kumar et al., 2018). They also found isotopic compositions to be more stable during the summer, similar to the dust collected at distal Barbados, reflecting a more stable dust source or consistent mixing of different sources during this time. Therefore, the measured Sr isotopic signal in the shipboard-collected aerosol samples is likely the result of the provenance of the dust, which can vary between the seasons, and also annually.

4.5. Examining possible contributions from Amazon River sediments

The westernmost mooring M4 (49 °W) is located in the vicinity of Amazon-River outflow, and therefore a possible sediment contribution may come from Amazon riverine lithogenic particles. Saharan dust is virtually the only source of lithogenic sediments to the deep sea in the eastern Atlantic Ocean, but west of the mid Atlantic ridge there is a large influence of riverine sediments from the Amazon and Orinoco rivers and nepheloid layers (Biscaye and Eittreim, 1977; Grousset and Biscaye, 2005). In two of the twenty-four sampling intervals, #12 (13-04-2013–29-04-2013) and #24 (22-10-2013–07-11-2013), very high deposition fluxes were observed (Van der Does et al., 2016; Korte et al., 2017), leading to question the origin of the lithogenic particles as Saharan dust only. Nutrients carried with the Amazon River outflow reached the sediment-trap sampling site and influenced phytoplankton productivity, resulting in increased coccolithophore fluxes (Guerreiro et al., 2017). The question remains if part of the lithogenic fraction found in the sediment-trap samples may originate from Amazon River sediments. Geochemical analysis of these samples and synchronous samples at the easternmost mooring M1 (23 °W) could shed light on the provenance of the lithogenic fraction found in the sediment traps. To test the hypothesis of a possible influence of Amazon sediments to the sediment trap at M4, the data are compared to sediments collected from the Amazon Basin and the Bodélé Depression (Abouchami et al., 2013), and to suspended sediment load from two tributaries of the Amazon River; the Madeira and Solimoes Rivers (Viers et al., 2008).

The combination of Sr and Nd isotopes can give a better insight into the potential source areas of the deposited dust (Grousset and Biscaye, 2005; Scheuvens et al., 2013; Pourmand et al., 2014; Sharifi et al., 2018; Zhao et al., 2018). Sediments collected in the Amazon Basin (Abouchami et al., 2013) and from the Solimoes and Madeira Rivers (Viers et al., 2008) show different εNd – $^{87}Sr/^{86}Sr$ values than the Saharan dust samples (Fig. 3B) as collected by the sediment traps, via shipboard aerosol collection and the atmospheric dust sampled at Barbados (Pourmand et al., 2014; Bozlaker et al., 2018). The Solimoes River sediments have lower Sr isotopic values than the sediment-trap samples but similar values to the shipboard-collected aerosol samples. However, the Solimoes River sediments yield more radiogenic Nd isotopic values. The Madeira River sediments show more similar Nd isotopic values but more radiogenic Sr isotopic values compared to the various dust samples. The combination of both radiogenic isotopes clearly illustrates the difference between the Amazon-derived sediments and Saharan-dust samples. In contrast to the geochemical signatures found in South-American sediments, the samples collected from the Bodélé Depression (Abouchami et al., 2013) are more similar to the Saharan dust samples, although over a wide range for both Sr and Nd composition, and strengthens the hypothesis of a north African provenance dominating the Atlantic dust particles.

The REE concentration patterns can also be used to distinguish between different sources of lithogenic material. The REE patterns of the dust samples collected at Barbados (Pourmand et al., 2014) are nearly identical to the shipboard-collected aerosol samples (Fig. 5B). The sediment-trap samples also show similarities with the Barbados samples, and have an apparent enrichment of HREE (Fig. 5A). Between 1 and 3% of the REEs can be dissolved into seawater, with especially the middle REEs (Eu–Er) showing greater solubility than LREE and HREE (Greaves et al., 1994). This small amount of solubility may have slightly affected the middle REEs of sample M4-12 (Fig. 5A). The samples are also closely related to the samples collected from the Bodélé area (Abouchami et al., 2013), with a similar Eu-enrichment. The sediment-trap samples are also very similar to the aerosol samples collected over the Atlantic, as well as to the aerosol samples from Barbados, demonstrating that the dust fraction was effectively isolated from the marine samples. The similarity of REE patterns from sediment-trap samples from M1 and M4 already indicates a minimal influence of Amazon-derived sediments to the M4 samples, as these will never reach as far east as M1 without being sedimented to the ocean floor. At the same time, the REE profiles from the sediment traps differ greatly from those originating from the Amazon Basin, demonstrating the different origin of the sediments in the sediment-trap samples.

The difference with the sediments collected from the Amazon Basin

once again highlights the unlikely contribution from Amazon River sediments to the sediment-trap samples. The Amazon Basin sediments show depleted Middle REEs and enriched HREEs, making the samples distinctly different from the Saharan dust samples. However, the sediments collected from the two tributaries of the Amazon River, the Solimoes and Madeira River (Viers et al., 2008), show more similar REE concentration patterns to the Saharan dust samples, with an enrichment in Eu and no enrichment in HREEs, and even a HREE depletion for the Madeira River samples (Fig. 5A). The REE signature from the Amazon sediments is the result of LREE depletion due to salt-induced coagulation or river borne colloidal REEs in low salinity regimes, making them more fractionated (Sholkovitz, 1993). The Madeira and Solimoes rivers show less fractionation since these are more representative of upstream waters that did not experience mixing with the oceanic end member. Riverine sediments that would have traveled towards the sediment traps would be expected to show this fractionated REE signature, which is not present in the sediment-trap samples. Instead, the sediment traps show a small enrichment in HREEs compared to the aerosol samples, which is likely due to the influence of seawater REE signature; enriched in HREEs and depleted in LREEs (Elderfield, 1988; Sholkovitz, 1993).

4.6. REE anomalies

Ce anomalies of the aerosol samples are all positive (> 1), meaning similar to the continental crust (Sholkovitz, 1993). Positive Ce anomalies can be indicative of more zircon particles in the sample. Therefore, a positive Ce anomaly would be expected for Saharan dust samples, in contrast to the dissolved fraction that shows a negative Ce anomaly (Sholkovitz, 1993). The sediment-trap samples indeed all show negative Ce anomalies. However, while others have reported both positive and negative Eu anomalies for refractory fractions in sediment-trap samples (Tachikawa et al., 1997), all the samples from this study (aerosols, sediment-trap samples and Barbados samples) show positive Eu anomalies. The individual shipboard-collected aerosol samples seem to mostly group together for each sampling campaign, indicating this dust, sampled in close proximity not more than a day apart, likely has a stable source area.

The shipboard-collected aerosol samples show Sm-Nd model ages and La_N/Lu_N values similar to the aerosol samples collected at Barbados, and to sediments from the Bodélé depression. Contrastingly, the data differ greatly from sediments from the Madeira River and Amazon Basin, but are similar to sediments collected from the Solimoes River (Fig. 6D).

5. Conclusions

Our results do not show a systematic shift in Sr isotope composition with dust particle size as expected with changes in mineralogy of transported particles of progressively smaller size. We therefore hypothesize that a combination of particle size, related to transport distance and seasonal changes in dust transport, and changes in dust provenance should be considered when interpreting Sr isotope data in aerosols. Also the Nd isotopic compositions do not show clear relations to dust particle size, in line with previous results (Feng et al., 2009; Meyer et al., 2011). The relation to particle size as shown by the Hf isotopic composition is due to the zircon effect (Patchett et al., 1984; Aarons et al., 2013), as coarse-grained zircon particles are deposited close to the source, thereby progressively shifting the Hf isotopic composition of aerosols to more radiogenic values with distance from the source. Therefore, the Hf isotopic composition would only be suited for source identification when the dust is sampled in a single location, as the Hf isotopic composition is influenced by dust transport distance and particle size. When sampling in a single location, the Hf isotopic composition would only change as a function of changing sources, and not as a result of changing sampling locations.

The similarity of REE patterns and isotopic composition of the

samples from the distal sampling station M4 to the most proximal station M1 shows that Saharan dust dominates the terrigenous fraction all along the trans-Atlantic transect, and that the contribution of Amazon-derived sediments to the sediment-traps is minimal. The REE patterns of the sediment-trap samples and shipboard-collected aerosols are also similar to dust collected at Barbados and samples from the Bodélé Depression in Chad, and very different from Amazon basin sediments. This makes an Amazon origin of the lithogenic particles again unlikely. The REE data from two tributaries of the Amazon River, however, are not conclusive, albeit expected to become more fractionated downstream. These are excluded as potential sediment sources to the sediment-trap samples due to their different Sr-Nd isotopic signatures to the Saharan dust samples. Rather, the combination of Sr-Nd isotopes of the dust samples point to a source somewhere in the western region of northern Africa.

Sediment-trap samples that sampled at the same time interval (M1-12 and M4-12; M1-24 and M4-24) are expected to have the same dust source, as they were sampled at the same time and at the same water depth. This is because the source of the dust within one dust cloud can be assumed to remain the same downwind, as no additional dust is added to the dust cloud while crossing the Atlantic Ocean. However, the composition of the dust can slightly change downwind due to the sedimentation of coarser and heavier particles earlier during transit, although the source remains the same. Differences in isotopic signature are therefore related to transport distance as a result of size and mineralogy fractionation, and not to changes in dust provenance for that particular time interval. The same can be seen when comparing the sediment-trap samples to dust collected even further downwind at Barbados in the same sampling year. However, the shipboard-collected aerosol samples from individual sampling campaigns are collected in close proximity to each other with little time between them, and also show a similar compositional variability as the sediment-trap samples, which is apparently a normal range for the average isotopic composition of a dust cloud. Sampling on an even higher resolution in both space and time should give more insights on the reproducibility of such shipboard-collected aerosols, and the short-term evolution of the (average) isotopic composition of a dust cloud. In interpreting the geochemical composition of aerosols, the influence of source provenance based on soil composition, sampling season and year, transport mechanisms, distance from the source and thereby particle size and mineralogy segregation should be considered.

Data availability

The data have been stored in Pangaea, at: https://doi.pangaea.de/10.1594/PANGAEA.890901.

Appendix A. Supplementary data

Supplementary data associated with this article can be found, in the online version, at https://doi.org/10.1016/j.aeolia.2018.06.001.

References

Aarons, S.M., Aciego, S.M., Gleason, J.D., 2013. Variable Hf Sr Nd radiogenic isotopic compositions in a saharan dust storm over the atlantic: implications for dust flux to oceans, ice sheets and the terrestrial biosphere. Chem. Geol. 349–350, 18–26.

Abouchami, W., Nathe, K., Kumar, A., Galer, S.J.G., Jochum, K.P., Williams, E., Horbe, A.M.C., Rosa, J.W.C., Balsam, W., Adams, D., Mezger, K., Andreae, M.O., 2013. Geochemical and isotopic characterization of the bodele depression dust source and implications for transatlantic dust transport to the Amazon Basin. Earth Planet. Sci. Lett. 380, 112–123.

Armitage, S.J., Bristow, C.S., Drake, N.A., 2015. West African monsoon dynamics inferred from abrupt fluctuations of Lake Mega-Chad. PNAS 112 (28), 8543–8548.

Armstrong, R.A., Lee, C., Hedges, J.I., Honjo, S., Wakeham, S.G., 2002. A new, mechanistic model for organic carbon fluxes in the ocean based on the quantitative association of Poc with Ballast Minerals. Deep Sea Res. Part II 49 (1–3), 219–236.

Atkinson, J.D., Murray, B.J., Woodhouse, M.T., Whale, T.F., Baustian, K.J., Carslaw, K.S., Dobbie, S., O'Sullivan, D., Malkin, T.L., 2013. The importance of feldspar for ice nucleation by mineral dust in mixed-phase clouds. Nature 498 (7454), 355–358.

Bagnold, R.A., 1941. The Physics of Blown Sand and Desert Dunes. Methuen, London.

Bayon, G., Burton, K.W., Soulet, G., Vigier, N., Dennielou, B., Etoubleau, J., Ponzevera, E., German, C.R., Nesbitt, R.W., 2009. Hf and Nd isotopes in marine sediments: constraints on global silicate weathering. Earth Planet. Sci. Lett. 277 (3–4), 318–326.

Biscaye, P.E., Eittreim, S.L., 1977. Suspended particulate loads and transports in the Nepheloid Layer of the Abyssal Atlantic Ocean. Mar. Geol. 23 (1), 155–172.

Bouvier, A., Vervoort, J.D., Patchett, P.J., 2008. The Lu–Hf and Sm–Nd isotopic composition of Chur: constraints from unequilibrated chondrites and implications for the bulk composition of terrestrial planets. Earth Planet. Sci. Lett. 273 (1), 48–57.

Bozlaker, A., Prospero, J.M., Price, J., Chellam, S., 2018. Linking barbados mineral dust aerosols to North African sources using elemental composition and radiogenic Sr, Nd, and Pb isotope signatures. Atmospheres 123 (2), 1384–1400.

Bressac, M., Guieu, C., Doxaran, D., Bourrin, F., Desboeufs, K., Leblond, N., Ridame, C., 2014. Quantification of the lithogenic carbon pump following a simulated dust-deposition event in large mesocosms. Biogeosciences 11 (4), 1007–1020.

Caquineau, S., Gaudichet, A., Gomes, L., Magonthier, M.C., Chatenet, B., 1998. Saharan dust: clay ratio as a relevant tracer to assess the origin of soil-derived aerosols. Geophys. Res. Lett. 25 (7), 983–986.

Castillo, S., Moreno, T., Querol, X., Alastuey, A., Cuevas, E., Herrmann, L., Mounkaila, M., Gibbons, W., 2008. Trace element variation in size-fractionated African Desert Dusts. J. Arid Environ. 72 (6), 1034–1045.

Chouza, F., Reitebuch, O., Benedetti, A., Weinzierl, B., 2016. Saharan dust long-range transport across the Atlantic studied by an airborne doppler wind lidar and the Macc Model: Atmos. Chem. Phys. 16 (18), 11581–11600.

Dasch, E.J., 1969. Strontium isotopes in weathering profiles, deep-sea sediments, and sedimentary rocks. Geochim. Cosmochim. Acta 33 (12), 1521–1552.

Dauphas, N., Pourmand, A., 2015. Thulium anomalies and rare earth element patterns in meteorites and earth: nebular fractionation and the nugget effect. Geochim. Cosmochim. Acta 163, 234–261.

De Baar, H.J.W., Bacon, M.P., Brewer, P.G., Bruland, K.W., 1985. Rare earth elements in the Pacific and Atlantic Oceans. Geochim. Cosmochim. Acta 49 (9), 1943–1959.

De Deckker, P., Abed, R.M.M., de Beer, D., Hinrichs, K.U., O'Loingsigh, T., Schefuss, E., Stuut, J.B.W., Tapper, N.J., van der Kaars, S., 2008. Geochemical and microbiological fingerprinting of Airborne Dust That Fell in Canberra, Australia, in October 2002. Geochem. Geophys. Geosyst. 9.

Elderfield, H., 1988. The oceanic chemistry of the rare-earth elements. Philos. Trans. R. Soc. London, Ser. A 325 (1583), 105–126.

Elderfield, H., Greaves, M.J., 1982. The rare earth elements in seawater. Nature 296 (5854), 214–219.

Feng, J.-L., Zhu, L.-P., Zhen, X.-L., Hu, Z.-G., 2009. Grain size effect on Sr and Nd isotopic compositions in eolian dust: implications for tracing dust provenance and Nd model age. Geochem. J. 43 (2), 123–131.

Friese, C.A., van der Does, M., Merkel, U., Iversen, M.H., Fischer, G., Stuut, J.-B.W., 2016. Environmental factors controlling the seasonal variability in particle size distribution of modern saharan dust deposited off cape blanc. Aeolian Res. 22, 165–179.

Friese, C.A., van Hateren, J.A., Vogt, C., Fischer, G., Stuut, J.B.W., 2017. Seasonal provenance changes in present-day Saharan dust collected in and off mauritania. Atmos. Chem. Phys. 17 (16), 10163–10193.

Goldstein, S.L., O'Nions, R.K., Hamilton, P.J., 1984. A Sm-Nd isotopic study of atmospheric dusts and particulates from major river systems. Earth Planet. Sci. Lett. 70 (2), 221–236.

Greaves, M.J., Statham, P.J., Elderfield, H., 1994. Rare earth element mobilization from marine atmospheric dust into seawater. Mar. Chem. 46 (3), 255–260.

Griffin, D.W., 2007. Atmospheric movement of microorganisms in clouds of desert dust and implications for human health. Clin. Microbiol. Rev. 20 (3), 459–477.

Grousset, F.E., Biscaye, P.E., 2005. Tracing dust sources and transport patterns using Sr, Nd and Pb isotopes. Chem. Geol. 222 (3), 149–167.

Grousset, F.E., Biscaye, P.E., Zindler, A., Prospero, J., Chester, R., 1988. Neodymium isotopes as tracers in marine sediments and aerosols: North Atlantic. Earth Planet. Sci. Lett. 87 (4), 367–378.

Guerreiro, C.V., Baumann, K.H., Brummer, G.J.A., Fischer, G., Korte, L.F., Merkel, U., Sá, C., de Stigter, H., Stuut, J.B.W., 2017. Coccolithophore fluxes in the open tropical North Atlantic: influence of thermocline depth, Amazon Water, and Saharan Dust. Biogeosciences 14 (20), 4577–4599.

Handley, H.K., Turner, S., Afonso, J.C., Dosseto, A., Cohen, T., 2013. Sediment residence times constrained by uranium-series isotopes: a critical appraisal of the comminution approach. Geochim. Cosmochim. Acta 103, 245–262.

Hoskin, P.W.O., Schaltegger, U., 2003. The composition of zircon and igneous and metamorphic petrogenesis. Chapter 2, Vol. 53 In: Hanchar, J.M., Hoskin, P.W.O. (Eds.), Zircon. Reviews in Mineralogy and Geochemistry. Mineralogical Society of America, Washington, DC, pp. 27–62.

Huneeus, N., Schulz, M., Balkanski, Y., Griesfeller, J., Prospero, J., Kinne, S., Bauer, S., Boucher, O., Chin, M., Dentener, F., Diehl, T., Easter, R., Fillmore, D., Ghan, S., Ginoux, P., Grini, A., Horowitz, L., Koch, D., Krol, M.C., Landing, W., Liu, X., Mahowald, N., Miller, R., Morcrette, J.J., Myhre, G., Penner, J., Perlwitz, J., Stier, P., Takemura, T., Zender, C.S., 2011. Global dust model intercomparison in Aerocom Phase I. Atmos. Chem. Phys. 11 (15), 7781–7816.

Kandler, K., SchÜTz, L., Deutscher, C., Ebert, M., Hofmann, H., JÄCkel, S., Jaenicke, R., Knippertz, P., Lieke, K., Massling, A., Petzold, A., Schladitz, A., Weinzierl, B., Wiedensohler, A., Zorn, S., Weinbruch, S., 2009. Size distribution, mass concentration, chemical and mineralogical composition and derived optical parameters of the boundary layer aerosol at Tinfou, Morocco, During Samum 2006. Tellus B 61 (1), 32–50.

Kandler, K., Schütz, L., Jäckel, S., Lieke, K., Emmel, C., Müller-Ebert, D., Ebert, M., Scheuvens, D., Schladitz, A., Šegvić, B., Wiedensohler, A., Weinbruch, S., 2011. Ground-based off-line aerosol measurements at Praia, Cape Verde, during the Saharan mineral dust experiment: microphysical properties and mineralogy. Tellus B 63 (4), 459–474.

Koren, I., Kaufman, Y.J., Washington, R., Todd, M.C., Rudich, Y., Martins, J.V., Rosenfeld, D., 2006. The Bodele depression: a single spot in the Sahara that provides most of the mineral dust to the Amazon Forest. Environ. Res. Lett. 1, 1.

Korte, L.F., Brummer, G.J.A., van der Does, M., Guerreiro, C.V., Hennekam, R., van Hateren, J.A., Jong, D., Munday, C.I., Schouten, S., Stuut, J.B.W., 2017. Downward particle fluxes of biogenic matter and saharan dust across the Equatorial North Atlantic. Atmos. Chem. Phys. 17 (9), 6023–6040.

Kumar, A., Abouchami, W., Galer, S.J.G., Singh, S.P., Fomba, K.W., Prospero, J.M., Andreae, M.O., 2018. Seasonal radiogenic isotopic variability of the African dust outflow to the Tropical Atlantic Ocean and across to the Caribbean. Earth Planet. Sci. Lett. 487, 94–105.

Kuznetsov, A.B., Semikhatov, M.A., Gorokhov, I.M., 2012. The Sr isotope composition of the World Ocean, Marginal and Inland Seas: implications for the Sr isotope stratigraphy. Stratigr. Geol. Correl. 20 (6), 501–515.

Li-Jones, X., Prospero, J.M., 1998. Variations in the size distribution of non-sea-salt sulfate aerosol in the marine boundary layer at Barbados: impact of African Dust. J. Geophys. Res. Atmos. 103 (D13), 16073–16084.

Maher, B.A., Prospero, J.M., Mackie, D., Gaiero, D., Hesse, P.P., Balkanski, Y., 2010. Global connections between aeolian dust, climate and ocean biogeochemistry at the present day and at the last glacial maximum. Earth Sci. Rev. 99 (1–2), 61–97.

Martin, J.H., Fitzwater, S.E., 1988. Iron-deficiency limits phytoplankton growth in the Northeast Pacific Subarctic. Nature 331 (6154), 341–343.

Meyer, I., Davies, G.R., Stuut, J.-B.W., 2011. Grain size control on Sr-Nd isotope provenance studies and impact on paleoclimate reconstructions: an example from deep-sea sediments offshore Nw Africa. Geophys. Geosyst. 12 (3).

Meyer, I., Davies, G.R., Vogt, C., Kuhlmann, H., Stuut, J.-B.W., 2013. Changing rainfall patterns in Nw Africa since the Younger Dryas. Aeolian Res. 10, 111–123.

Moreno, T., Querol, X., Castillo, S., Alastuey, A., Cuevas, E., Herrmann, L., Mounkaila, M., Elvira, J., Gibbons, W., 2006. Geochemical variations in aeolian mineral particles from the Sahara-Sahel dust corridor. Chemosphere 65 (2), 261–270.

Morman, S.A., Plumlee, G.S., 2014. Dust and human health. Chapter 15 In: Knippertz, P., Stuut, J.B.W. (Eds.), Mineral Dust, a Key Player in the Earth System. Springer Science +Business Media, Dordrecht, pp. 385–409.

Muhs, D.R., 2013. The geologic records of dust in the quaternary. Aeolian Res. 9, 3–48.

Muhs, D.R., Budahn, J.R., Prospero, J.M., Carey, S.N., 2007. Geochemical evidence for African dust inputs to soils of Western Atlantic Islands: Barbados, the Bahamas, and Florida. J. Geophys. Res. 112 (F2).

Mulitza, S., 2005. Climate History and Sedimentation Processes Off Nw Africa – Cruise No. M65 – June 1 – August 10, 2005 – Dakar (Senegal) – Las Palmas (Spain). Available from: https://Www.Tib.Eu/En/Search/Id/Awi%3adoi~10.2312%252fcr_M65/.

Nicholson, S.E., 2000. The nature of rainfall variability over Africa on time scales of decades to Millenia. Global Planet. Change 26 (1–3), 137–158.

Patchett, P.J., White, W.M., Feldmann, H., Kielinczuk, S., Hofmann, A.W., 1984. Hafnium/rare earth element fractionation in the sedimentary system and crustal recycling into the Earth's mantle. Earth Planet. Sci. Lett. 69 (2), 365–378.

Pourmand, A., Dauphas, N., 2010. Distribution coefficients of 60 elements on Todga resin: application to Ca, Lu, Hf, U and Th Isotope Geochemistry. Talanta 81 (3), 741–753.

Pourmand, A., Dauphas, N., Ireland, T.J., 2012. A novel extraction chromatography and Mc-Icp-Ms technique for rapid analysis of Ree, Sc and Y: revising Ci-Chondrite and Post-Archean Australian Shale (Paas) Abundances. Chem. Geol. 291, 38–54.

Pourmand, A., Prospero, J.M., Sharifi, A., 2014. Geochemical fingerprinting of transAtlantic African dust based on radiogenic Sr-Nd-Hf isotopes and rare earth element anomalies. Geology 42 (8), 675–678.

Prospero, J.M., Bonatti, E., Schubert, C., Carlson, T.N., 1970. Dust in Caribbean atmosphere traced to an African dust storm. Earth Planet. Sci. Lett. 9 (3), 287–293.

Prospero, J.M., Ginoux, P., Torres, O., Nicholson, S.E., Gill, T.E., 2002. Environmental characterization of global sources of atmospheric soil dust identified with the Nimbus 7 total ozone mapping spectrometer (Toms) absorbing aerosol product. Rev. Geophys. 40 (1).

Prospero, J.M., Lamb, P.J., 2003. African droughts and dust transport to the caribbean: climate change implications. Science 302 (5647), 1024–1027.

Prospero, J.M., Nees, R.T., 1977. Dust concentration in atmosphere of equatorial North-Atlantic – possible relationship to Sahelian drought. Science 196 (4295), 1196–1198.

Ryder, C.L., Highwood, E.J., Rosenberg, P.D., Trembath, J., Brooke, J.K., Bart, M., Dean,

A., Crosier, J., Dorsey, J., Brindley, H., Banks, J., Marsham, J.H., McQuaid, J.B., Sodemann, H., Washington, R., 2013. Optical properties of Saharan dust aerosol and contribution from the coarse mode as measured during the Fennec 2011 aircraft campaign. Atmos. Chem. Phys. 13 (1), 303–325.

Scheuvens, D., Schütz, L., Kandler, K., Ebert, M., Weinbruch, S., 2013. Bulk composition of Northern African dust and its source sediments — a compilation. Earth Sci. Rev. 116, 170–194.

Schreuder, L.T., Stuut, J.-B.W., Korte, L.F., Sinninghe Damsté, J.S., Schouten, S., 2018. Aeolian transport and deposition of plant wax N-Alkanes across the Tropical North Atlantic Ocean. Org. Geochem. 115 (Suppl. C), 113–123.

Schweitzer, M.D., Calzadilla, A.S., Salamo, O., Sharifi, A., Kumar, N., Holt, G., Campos, M., Mirsaeidi, M., 2018. Lung health in Era of climate change and dust storms. Environ. Res. 163, 36–42.

Sharifi, A., Murphy, L.N., Pourmand, A., Clement, A.C., Canuel, E.A., Naderi Beni, A., Lahijani, H.A.K., Delanghe, D., Ahmady-Birgani, H., 2018. Early-holocene greening of the Afro-Asian dust belt changed sources of mineral dust in West Asia. Earth Planet. Sci. Lett. 481, 30–40.

Sholkovitz, E.R., 1993. The geochemistry of rare earth elements in the Amazon River Estuary. Geochim. Cosmochim. Acta 57 (10), 2181–2190.

Stuut, J.-B., Boersen, B., Brück, H.M., Hansen, A., Koster, B., van der Does, M., Witte, Y., 2012. Cruise Report Rv Meteor M89, Traffic I: Transatlantic Fluxes of Saharan Dust. 3 – 25 October 2012. Available from http://Melia.Nioz.Nl/Public/Dmg/Rpt/Crs/M89. Pdf.

Stuut, J.-B., Brummer, G.J.A., Van der Does, M., Friese, C., Geerken, E., van der Heide, R., Korte, L., Koster, B., Metcalfe, B., Munday, C. I., van Ooijen, J., Siccha, M., Veldhuizen, R., de Visser, J.-D., Witte, Y., Wuis, L., 2013. Cruise Report Rv Pelagia 64pe378, Traffic Ii: Transatlantic Fluxes of Saharan Dust. 9 November – 6 December 2013. Available from: http://Melia.Nioz.Nl/Public/Dmg/Rpt/Crs/64pe378.Pdf.

Stuut, J.-B., Witte, Y., de Visser, J.-D., Boersen, B., Koster, B., Bakker, K., Laan, P., van der Does, M., Korte, L., Munday, C. I., and van Hateren, H., 2015. Cruise Report Rv Pelagia 64pe395, Traffic Iii: Transatlantic Fluxes of Saharan Dust. 11 January – 6 February 2015. Available from: http://Melia.Nioz.Nl/Public/Dmg/Rpt/Crs/64pe395.Pdf.

Stuut, J.-B., Zabel, M., Ratmeyer, V., Helmke, P., Schefuss, E., Lavik, G., Schneider, R.,

2005. Provenance of present-day Eolian dust collected off Nw Africa. J. Geophys. Res. Atmos. 110, D04202.

Tachikawa, K., Handel, C., Dupré, B., 1997. Distribution of rare earth elements and neodymium isotopes in settling particulate material of the Tropical Atlantic Ocean (Eumeli Site). Deep Sea Res. Part I 44 (11), 1769–1792.

Thomas, J.B., Bodnar, R.J., Shimizu, N., Chesner, C.A., 2003. Melt inclusions in zircon. Rev. Mineral. Geochem. 53 (1), 63–87.

Van der Does, M., Korte, L.F., Munday, C.I., Brummer, G.J.A., Stuut, J.B.W., 2016. Particle size traces modern Saharan dust transport and deposition across the equatorial North Atlantic. Atmos. Chem. Phys. 16 (21), 13697–13710.

Van der Jagt, H., Friese, C., Stuut, J.B., Fischer, G., Iversen, M., 2018. The ballasting effect of saharan dust deposition on aggregate dynamics and carbon export: aggregation, settling and scavenging of marine snow. Limnol. Oceanogr.

Viers, J., Roddaz, M., Filizola, N., Guyot, J.-L., Sondag, F., Brunet, P., Zouiten, C., Boucayrand, C., Martin, F., Boaventura, G.R., 2008. Seasonal and provenance controls on Nd–Sr isotopic compositions of amazon rivers suspended sediments and implications for Nd and Sr fluxes exported to the Atlantic Ocean. Earth Planet. Sci. Lett. 274 (3–4), 511–523.

Washington, R., Todd, M.C., Lizcano, G., Tegen, I., Flamant, C., Koren, I., Ginoux, P., Engelstaedter, S., Bristow, C.S., Zender, C.S., Goudie, A.S., Warren, A., Prospero, J.M., 2006. Links between topography, wind, deflation, lakes and dust: the case of the Bodélé Depression, Chad. Geophys. Res. Lett. 33 (9), L09401.

Weill, D.F., Drake, M.J., 1973. Europium anomaly in Plagioclase Feldspar: experimental results and semiquantitative model. Science 180 (4090), 1059–1060.

Wilcox, E.M., Lau, K.M., Kim, K.-M., 2010. A Northward shift of the North Atlantic ocean intertropical convergence zone in response to summertime saharan dust outbreaks. Geophys. Res. Lett. 37 (4), L04804.

Yu, H., Chin, M., Bian, H., Yuan, T., Prospero, J.M., Omar, A.H., Remer, L.A., Winker, D.M., Yang, Y., Zhang, Y., Zhang, Z., 2015. Quantification of trans-atlantic dust transport from seven-year (2007–2013) record of Calipso Lidar measurements. Remote Sens. Environ. 159, 232–249.

Zhao, W., Balsam, W., Williams, E., Long, X., Ji, J., 2018. Sr–Nd–Hf isotopic fingerprinting of transatlantic dust derived from North Africa. Earth Planet. Sci. Lett. 486, 23–31.